End-to-end Full-Stack Drone Measurements: A Case Study Using AERPAW

Matteo Drago*, Anıl Gürses°, Robert W. Heath Jr.°, Mihail L. Sichitiu°, Michele Zorzi*
*Department of Information Engineering, University of Padova, Italy. E-mail: {dragomat, zorzi}@dei.unipd.it
°Department of Electrical and Computer Engineering, North Carolina State University, Raleigh, NC, USA
E-mail: {agurses, rwheathjr, mlsichit}@ncsu.edu

2023 IEEE International Conference on Communications Workshops (ICC Workshops) | 979-8-3503-3307-7/23/$31.00 ©2023 IEEE | DOI: 10.1109/ICCWORKSHOPS57953.2023.10283735

***Abstract*—While a lot of studies have been made to include drone communications in the 5th Generation of Mobile Networks (5G), it is still arguable how reliably current air-to-ground infrastructures can perform. To apply a further boost to this research direction, the National Science Foundation (NSF) recently funded the Aerial Experimentation Research Platform for Advanced Wireless (AERPAW) for the creation of a high-end publicly available testbed. Considering the current lack in the literature of experimental studies carried out with open testbeds, in this paper we target two contributions. First, we use AERPAW for the end-to-end evaluation of the performance of an emulated Uplink (UL) traffic between an Unmanned Aerial Vehicle (UAV) and a Fixed Node (FN), connected through an open source LTE network software (srsRAN). Second, in addition to providing a thorough analysis of the results obtained from our experiments, we made our testbed's configuration files and collected dataset available to the public, to provide a reference for future research on UAV communication, enabled by AERPAW.**

***Index Terms*—AERPAW, UAV, SDR, LTE**

I. Introduction

In the last decade, Unmanned Aerial Vehicles (UAVs) have been applied to diverse use cases, such as: public safety tasks (e.g., event surveillance or, more recently, monitoring of social distancing protocols), consumer photography and entertainment (e.g., professional video recordings for moviemakers), business operations (e.g., logistic services being promoted by Amazon or UPS) and smart farming application (e.g., increase of the field productivity through image collection and analysis). According to estimates provided in [1], in fact, the UAVs market is expected to grow from 30 billion USD in 2022 up to 279 billion USD by 2032. Most of these applications benefit from a high quality communication link to a ground station. From the standardization point of view, the IEEE released the 802.11ah amendment to provide longer range and lower power connectivity to Wi-Fi networks [2], while the 3rd Generation Partnership Project (3GPP) is in the process of adding features to cellular systems to support the communication among drones[1] and between drones and other network elements [3].

Prototyping is an essential ingredient in developing the next generation of heterogeneous networks. In this field, in particular, there have been various experimental studies, including: pathloss measurements, small-scale fading characterization, analysis on the impact of mobility in air-to-ground links, and optimization of the antenna position on the drone's frame. However, a major challenge that emerged from prior works in the literature is reproducibility. Recently, the National Science Foundation (NSF) funded the Aerial Experimentation Research Platform for Advanced Wireless (AERPAW), an openly available experimental setup to enable advanced research on beyond 5G technologies, in particular in the context of aerial communication. A key feature of the testbed is that experimenters can remotely test and tune their algorithms to better reflect the challenges posed by real-world scenarios, while their experiments are carried out by on-field operators.

Our paper makes the following two contributions to the research community:

- We carry out an end-to-end full-stack measurement campaign with AERPAW between a UAV, acting as a User Equipment (UE), and a Fixed Node (FN), acting as an evolved Node Base (eNB). From our experiments we observe that standard communication protocols are not a good fit for these new scenarios characterized by a high channel variability, leading to fluctuating available bitrate and high packet loss.
- We provide a detailed explanation of the experiments' workflow, to allow other researchers to replicate our study and iterate on top of it. Moreover, in [4] we release the necessary files to configure AERPAW's Virtual Machines (VMs), Software Defined Radios (SDRs) and vehicles, along with the collected datasets.

II. Drones in Telecommunications: An Introduction

Studies of strategies on how to make UAVs communicate efficiently gained momentum in the last two decades, along with the rise of mobile networks. The authors of [5], [6] outline several challenges in this field such as, for example: stringent control and payload data requirements to be satisfied, the need for AI-based approaches for mobility management and UAV-aware network design, efficient antenna design, and beam-selection algorithms.

In general, we outline three main research topics: (i) efficient integration of SDRs to design wireless drones; (ii) creation of emulation tools to model the UAV environment

[1]In the context of this paper, we will use the terms drone and UAV interchangeably.

Authorized licensed use limited to: Northeastern University. Downloaded on June 26,2024 at 16:47:37 UTC from IEEE Xplore. Restrictions apply.

without the need to build the actual system; and (iii) the study of signal propagation in air-to-ground and drone-to-drone scenarios.

Integrating SDRs and UAVs: The authors of [7] built a GSM relay system to be deployed on a UAV, to provide cellular coverage in scenarios where cellular systems are damaged or malfunctioning. Another work [8] has developed an aerial base station prototyping platform called SkyCell. It provides a framework that offers control of the network and mobility of the UAV.

Emulation of drone networks: The authors in [9] designed a Radio Frequency (RF) Software in the Loop (SITL) channel emulator with I/Q sample fidelity, that aims at being a prototyping tool for the deployment of real software-defined drone networks. Another prototyping emulation environment, uavEE, was proposed in [10] and released as open source. Besides making it possible to interface the emulator with existing flight simulators, the authors developed a data driven power model and validated it, along with the emulator, on a real UAV flight.

Propagation studies: The work in [11] demonstrates through air-to-air measurements that the body of the drone can indeed affect the received power across various antenna orientations and positions and act as a local scatterer. In [12], the authors characterize air-to-ground wireless channels between UAV platforms and terrestrial users in practical Line-of-Sight (LoS) and Non-Line-of-Sight (NLoS) scenarios across a limited range of carrier frequencies below 6 GHz. Instead, the authors of [12] designed an IEEE 802.11-like signaling mechanism to feed back Channel State Information (CSI) for both wideband and beamformed transmissions, and they performed tests at different heights and distances.

Our proposal: Even though AERPAW is a newborn testbed, a lot of research has already been carried out, mostly focused on high-level preliminary performance evaluations, UAV detection using RF fingerprints, or propagation measurements at mmWave [13]–[15]. Our work is the first that uses AERPAW to study the performance of UAVs mobile networks with an end-to-end and full-stack approach. In addition, by releasing the code and the collected dataset, we aim to stimulate new studies in this field, allowing researchers to use our contribution as a baseline.

Fig. 1: PN with USRP B210 and 4 stub antennas, mounted on a UAV

III. Experiments

The experiments described in the following have been carried out using the AERPAW testbed in Lake Wheeler, Raleigh, NC. The Lake Wheeler site offers a tower (variable height between ∼10 m and ∼20 m) equipped with 4 Universal Software Radio Peripherals (USRPs) and 6 omni-directional antennas that can operate between 1.7 GHz and 6 GHz. For our measurements, we used USRP B210 both at FN and Portable Nodes (PNs), due to its wide range of features compared to USRP B205mini.

With respect to the UAV, the AERPAW team designed and built a custom hexacopter, described in detail in [16]. The hexacopter carries a payload that consists of: the radio front-end, a USRP B210, a USRP B205mini, and an Intel™ NUC with i7-10710U. Compared to the USRPs on the PN, the B205mini is used by AERPAW's operators for RF spectrum monitoring to avoid any harmful (or illegal) transmission that might arise from the experiment, while the B210 can be used by an experimenter and configured according to the measurements needs.

Despite the fact that the Lake Wheeler site has a negligible amount of RF noise when compared to more crowded or built-up areas, the RF front-end is needed to filter out some parts of the spectrum and amplify the transmitted/received signal. To this end, the deployed RF front-end is capable of (i) amplifying the received signal with a Low Noise Amplifier (LNA), (ii) blocking signals below 3 GHz and above 4.3 GHz with a Band Pass Filter (BPF), (iii) duplexing the receive chain into two parts for RF monitoring and experimenter's application. On the transmit chain, a Low Pass Filter (LPF) was used to filter out the signals above 4.4 GHz. Four stub antennas placed on the node with both horizontal and vertical polarization, that can operate at L-, S-, and C-band, are used. An example of a PN as the one just described is shown in Figure 1.

In addition to the abovementioned features, each PN is also capable of independently operating the vehicle through a MAVLink connection to the flight computer. To do so, before the experiment moves into the testbed and UAV, the experimenter designs a flight trajectory with a flight plan software such as QGroundControl [17] which is used in this experiment.

Regarding the experimental workflow in AERPAW, the overall process comprises two stages: (i) the emulation/development mode and (ii) the testbed mode. The emulation mode is the starting point for every experiment, as it provides different templates for AERPAW's testing sites. As of Phase 1, there are two preconfigured templates:

- 1 FN plus 1 PN at Lake Wheeler.
- 2 FNs at Centennial Campus.

The AERPAW platform creates 4 types of containers for each experiment which are Experiment Virtual Machine (E-VM), Control Virtual Machine (C-VM), Channel Emulator (CHEM) VM, and Operator Experiment Oversight (OEO) VM. E-VM consists of experimenter code and related logger services provided by the AERPAW platform. E-VM

Authorized licensed use limited to: Northeastern University. Downloaded on June 26,2024 at 16:47:37 UTC from IEEE Xplore. Restrictions apply.

is connected to C-VM over a virtual network for sending commands and receiving logs from the vehicle. According to the previous statement, C-VM is responsible for controlling the vehicle through the flight computer (or an SITL configuration, for the emulation case) using the MAVLink interface. The OEO VM is only used in emulation mode to execute commands such as arming the vehicle.

To provide a means of transferring signals between containers, ZMQ [18] is used to create a channel emulator and is placed into CHEM VM, as described in [13]. Besides the emulation of the wireless channel, it is also possible to emulate vehicles (Unmanned Ground Vehicle (UGV) and UAV) using the same software that will be eventually deployed on the devices, making the transition process from emulation mode to testbed easier. Once the development is done for the emulation mode, the experimenter submits their execution to the platform and the experiment is carried out by AERPAW operators.

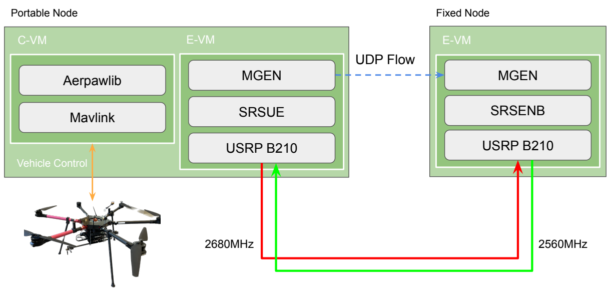

Fig. 2: Overview of the measurement setup

In this study, Uplink (UL) traffic is exchanged between the drone and the eNB, through the LTE network configured as shown in Figure 2. The main motivation behind using the LTE network is to stress the LTE performance on UAV communications and give an idea for possible future improvements. In the literature, the amount of studies available in quasi-realistic traffic model performance evaluation with LTE air-to-ground network is limited and LTE promises a good fit for low powered Internet of Things (IoT) devices in rural area applications. The setup that we built aims to show where possible improvements can be made in the LTE stack to enable air-to-ground communication systems, and we corroborate our vision with a set of measurements described in detail in Section IV. Traffic generation is handled with MGEN [19], an open source traffic generation software (more details on the emulated use case and the software configuration will be given in Section IV). To set up the LTE connectivity between the PN and the FN, the open source LTE software srsRAN [20] is used with 100 Physical Resource Block (PRB) configuration.

For a thorough performance evaluation, we designed our flights such that each consisted of three consecutive laps. When the drone is far away from the eNB and the estimated Signal-to-Interference-plus-Noise Ratio (SINR) drops, however, disconnections and reconnections may happen very often. During the first set of testing flights, we encountered a disconnection problem due to a bug in srsRAN, that was causing a reattachment failure on the UE side, making it impossible to conclude the experiment. To solve the problem, we developed a fix to the reattachment procedure following the 3GPP LTE specifications [21], allowing the UE to go into a cell search state upon a failure to reattach. The patched version of the code can be found at [22].

To summarize, all the required scripts for starting the experiment and the different traffic model files are included in [4], so that the experiments can be submitted and run by AERPAW operators without any changes. The vehicle script is necessary to transfer the flight plan to the PN and send the required commands to start the flight and follow the preplanned trajectory. While in our case the script is for the deployment of the UAV, the experiment can be completed with different vehicles (e.g., UGV) just by changing the trajectory parameters, or even without a vehicle entity if we are not interested in mobility. Note that it is also possible to deploy our solution on an independent testbed (different from AERPAW) with minor adjustments, such as: vehicle trajectory replanning and change of the destination IP address in MGEN setup files.

IV. Performance Evaluation

After a thorough planning and testing phase using the emulation tools provided by AERPAW, we proceeded with a measurement campaign with the setup described in Section III. In our experiments, we were interested in emulating the dissemination of real-time perception data generated from vehicles' onboard sensors like Light Detection and Ranging (LiDAR) to a remote entity (e.g., field operator, remote cloud controller). In fact, the use case that we wanted to replicate consists in the transmission of information for the study of rural areas, with applications such as monitoring of environmental phenomena, safety assistance in case of natural disasters, and crop analysis through extensive data collection.

Having considered the richness of information available in such scenarios, the transmission of sensor data requires a substantial amount of radio resources and could potentially congest the network. To tackle this issue, data compression and segmentation are often applied in order to reduce the size of raw data prior to transmission. For this reason, our application generates data based on the first-order statistics of the Kitti multi-modal dataset [23], extended to include the data compression pipeline proposed in [24]. The dataset provides the frame sizes (in Bytes) associated with a collected LiDAR point-cloud, both raw and after applying compression and/or semantic segmentation: the higher the level of shrinking, the smaller the size of a single packet.

We analyzed the dataset to obtain the average application rate (i.e., the rate at which the application is generating data towards the receiver) associated with each compression/segmentation option. To further clarify, if the application rate of a specific LiDAR mode is 16 Mbps, this translates into a corresponding data rate in MGEN. In all our cases the packet size was set to 8192B and, in a periodic time window of 100

Authorized licensed use limited to: Northeastern University. Downloaded on June 26,2024 at 16:47:37 UTC from IEEE Xplore. Restrictions apply.

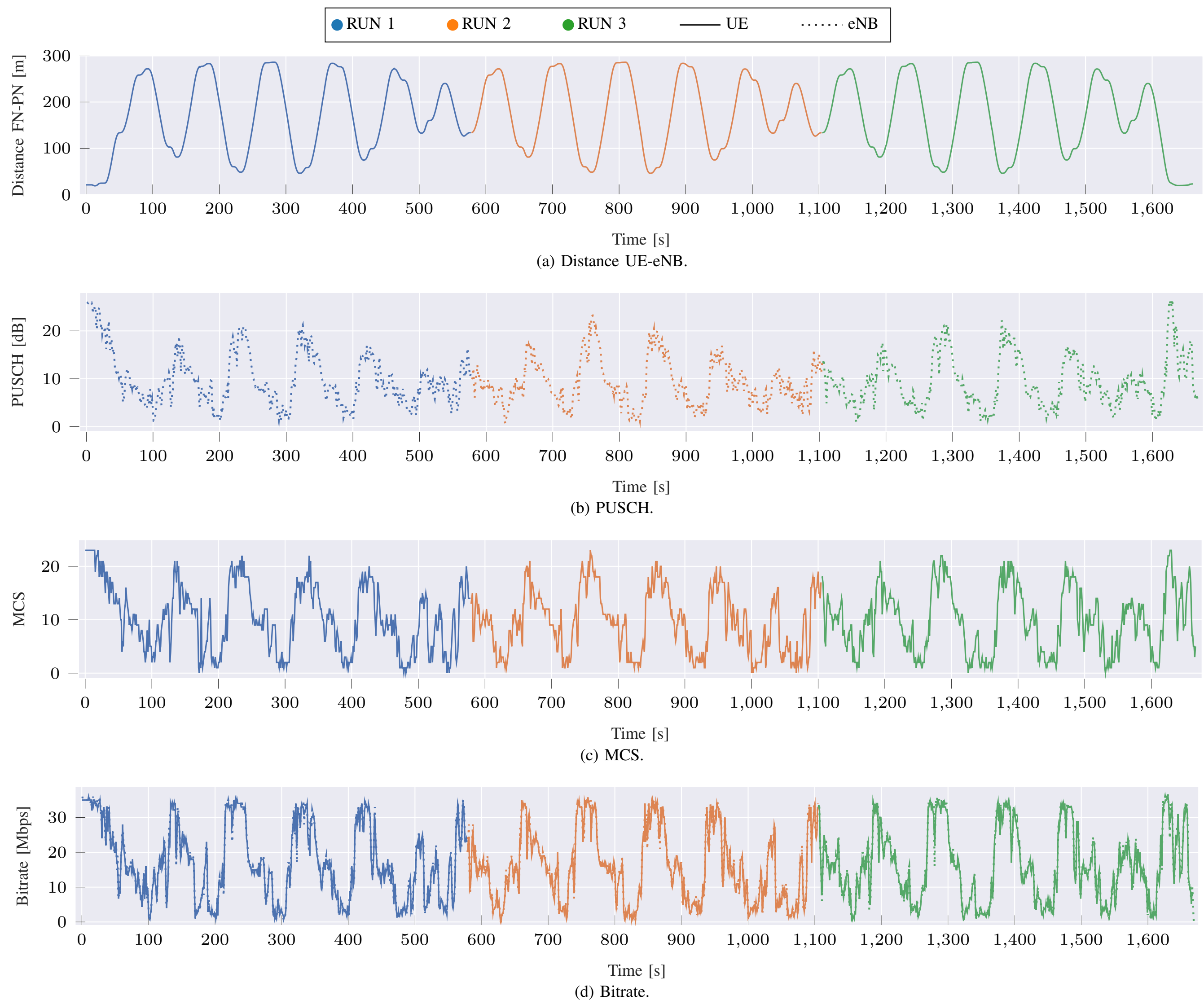

Fig. 3: Physical radio measurements on UE and eNB with aggregated target APP rate of ∼ 32Mbps.

ms with a 50% duty cycle, MGEN generates an equivalent number of packets to reach the target rate.

Since MGEN can create separate User Datagram Protocol (UDP) flows by specifying different sending/listening ports on the transmitting/receiving devices, we were able to test how resources were orchestrated among traffic flows. We evaluated the performance of the setup for the following three application sending strategies, each with a constant number of traffic sources and target sending bitrate, selected by those obtained from the analysis of [23], [24]:

- Single UL flow with a ∼16 Mbps target application rate.
- Two separate UL flows, each with a ∼8.3 Mbps target application rate.
- Two separate UL flows, each with a ∼16 Mbps target application rate.

As highlighted in the previous section, a single measurement consists of three distinct laps following a preplanned trajectory, each referred to as *run* in the following (i.e., for each application mode, we performed three runs). In this way, besides collecting more samples that could enable artificial intelligence approaches, we also wanted to study the consistency of the results obtained with the same parameters among distinct consecutive trials. The speed of the drone was set to 7 m/s, for a total of ∼25 minutes per experiment.

Figure 3 shows a set of results obtained at the Physical Layer (PHY) of UE and eNB, specifically when the source application was generating two separate flows, for a resulting aggregated traffic of ∼32 Mbps. Figure 3a depicts the distance between the vehicle and the FN throughout the experiment and was used to verify that the radio metrics were consistent and correlated with the PN movements. The SINR shown in Figure 3b measured at the eNB behaved as expected: the larger the distance, the lower its value (and vice versa). Conversely, the performance of the default Modulation and Coding Scheme

Authorized licensed use limited to: Northeastern University. Downloaded on June 26,2024 at 16:47:37 UTC from IEEE Xplore. Restrictions apply.

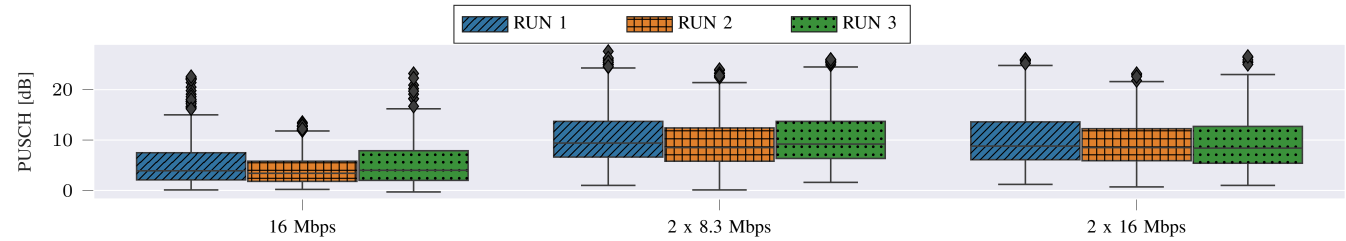

(a) SINR estimated at the eNB PUSCH.

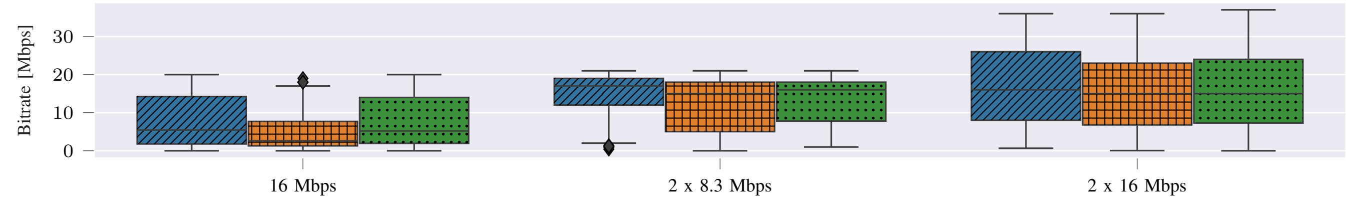

(b) RX PHY rate.

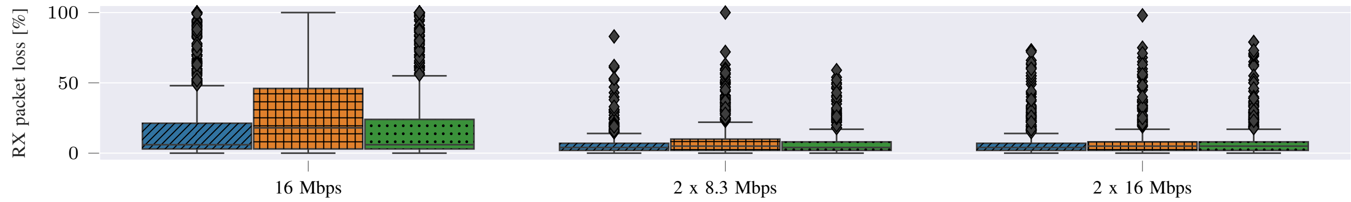

(c) RX PHY loss rate.

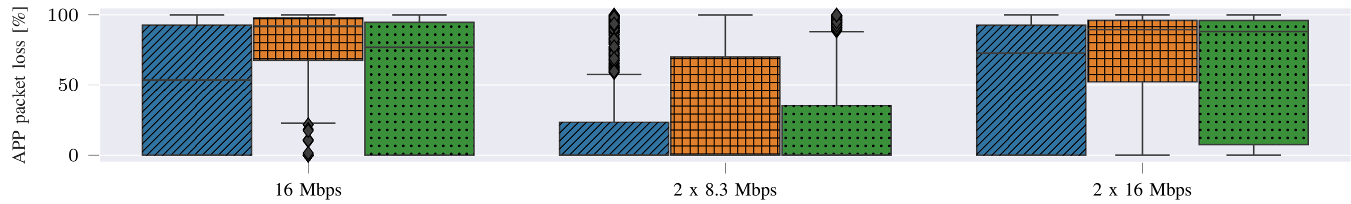

(d) RX application loss rate.

Fig. 4: Aggregated measurements for three runs and three offered traffic profiles for each run.

(MCS) selection strategy implemented by srsRAN is presented in Figure 3c. The algorithms strictly follow the SINR trend and quickly adapt to sudden SINR drops. However, while this behavior might be good in the case of resource-hungry applications, it is not ideal for QoS-oriented scenarios. In that case, it would be better to provide the user with a stable network output to the user rather than trying to always match the peak performance. It is clear from Figure 3d that a high MCS variability corresponds to an unstable bitrate, which eventually leads to high packet losses and delays.

To confirm the consistency of consecutive measurements, in Figure 4 we compare the boxplots of different metrics in distinct runs. Each box shows the median and the corresponding 25^{th} and 75^{th} percentiles of the dataset, while the whiskers extend to show the rest of the distribution with respect to the interquartile range. The points below or above the whiskers represent the measurements' outliers. Figure 4a shows that, besides the variability related to the drone going back and forth in the field, the SINR trend is consistent throughout the different runs, and the results in Figure 4b are an immediate consequence of that.

As highlighted in the previous sections, this study aims also at providing a bottom-up performance evaluation, including measurements of QoS parameters at the Application (APP) layer, based on the generated UDP flows. Specifically, Figures 4c and 4d show how the packet loss experienced at the receiver's PHY is reflected into an even higher loss at the APP. This is motivated by the fact that the big packets we are generating at the APP layer need to be fragmented before being sent through the channel. Based on how many packets reach the destination, the receiving APP might not be able to fully retrieve the original frame, which is consequently considered lost and contributes to up to 100% packet loss. This, along with the highly variable bitrate trend shown in Figure 3d, further stresses the need for adaptation algorithms to guarantee stable performance.

A. A Dataset Use-Case: Area Clustering

Finally, in Figure 5 we show how the value of SINR estimated at the eNB can be used to identify communication clusters. This information can be very useful both to know upfront, in order to tailor network algorithms using the GPS

Authorized licensed use limited to: Northeastern University. Downloaded on June 26,2024 at 16:47:37 UTC from IEEE Xplore. Restrictions apply.

coordinates of the vehicle as input, but also if used to analyze rural areas to understand how to disseminate eNBs to reach optimal radio coverage. In our analysis, shown in Figure 5, we used K-Means as a well-known clustering algorithm to find three distinct clusters (corresponding to bad, good, and excellent channel quality), and noticed that identifying these areas is not as easy as expected. Among other things, this can be due to the antenna orientation, which varies depending on the vehicle trajectory along with its own high-speed mobility. Another thing to notice is that, although we have multiple SINR points associated with the same GPS coordinates (thanks to the consecutive laps), we may find the same area being assigned to different clusters. This further confirms the high channel variability even at LoS and the need for tailored algorithms to guarantee stable performance.

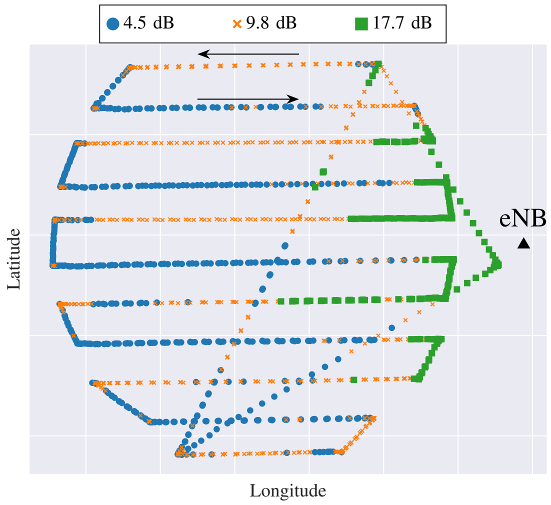

Fig. 5: Area clustering based on estimated SNR using K-Means

V. Conclusions

Despite the availability of detailed technical studies on the implementation of UAVs to enable air-to-ground communication, there are still a lot of problems that need to be addressed before witnessing a large scale deployment of this novel architecture. With the presented framework and published dataset, we aim at enabling researchers to help bridge this gap by: (i) using our work as a starting point to make further innovation with the AERPAW open testbed, and (ii) using the published dataset to bootstrap novel network solutions before deploying them in the field. In the future we are going to release a more extensive dataset that includes additional measurement campaigns using the UGV in addition to the UAV. Moreover, we also plan to design an adaptive data transmission algorithm that chooses between different compression modes and to test it on AERPAW.

References

[1] Fact.MR, "2017-2021 Demand Analysis of Drones vs. Future Outlook 2022-2032," Market Report, Feb. 2022. [Online]. Available: https://www.factmr.com/report/62/drone-market

[2] IEEE P802.11, *IEEE Standard for Information technology–Telecommunications and information exchange between systems - Local and metropolitan area networks–Specific requirements - Part 11: Wireless LAN Medium Access Control (MAC) and Physical Layer (PHY) Specifications Amendment 2: Sub 1 GHz License Exempt Operation*, Std., 2017.

[3] 3GPP, "Unmanned Aerial System (UAS) support in 3GPP," Technical Specification (TS) 22.125, Apr. 2022.

[4] SIGNET Laboratory and NC State University, "MGEN, srsRAN config files for AERPAW and analysis scripts." [Online]. Available: https://github.com/signetlabdei/aerpaw-experiments

[5] M. Mozaffari, W. Saad, M. Bennis, Y.-H. Nam, and M. Debbah, "A Tutorial on UAVs for Wireless Networks: Applications, Challenges, and Open Problems," *IEEE Commun. Surv. & Tut.*, vol. 21, no. 3, pp. 2334–2360, Mar. 2019.

[6] G. Geraci, A. Garcia-Rodriguez, M. M. Azari, A. Lozano, M. Mezzavilla, S. Chatzinotas, Y. Chen, S. Rangan, and M. Di Renzo, "What Will the Future of UAV Cellular Communications Be? A Flight from 5G to 6G," *IEEE Commun. Surv. & Tut.*, vol. 24, no. 3, pp. 1304–1335, May 2022.

[7] K. Guevara, M. Rodriguez, N. Gallo, G. Velasco, K. Vasudeva, and I. Guvenc, "UAV-based GSM network for public safety communications," in *SoutheastCon 2015*, 2015.

[8] L. Ferranti, L. Bonati, S. D'Oro, and T. Melodia, "SkyCell: A Prototyping Platform for 5G Aerial Base Stations," in *IEEE WoWMoM*, 2020, pp. 329–334.

[9] N. Mastronarde, D. Russell, Z. Guan, G. Sklivanitis, D. Pados, E. S. Bentley, and M. Medley, "RF-SITL: A Software-in-the-loop Channel Emulator for UAV Swarm Networks," in *IEEE WoWMoM*, 2022, pp. 489–494.

[10] M. Theile, O. D. Dantsker, R. Nai, and M. Caccamo, "uavEE: A Modular, Power-Aware Emulation Environment for Rapid Prototyping and Testing of UAVs," in *IEEE RTCSA*, 2018, pp. 217–224.

[11] M. Badi, J. Wensowitch, D. Rajan, and J. Camp, "Experimental evaluation of antenna polarization and elevation effects on drone communications," in *Proc. of ACM MSWIM*. New York, NY, USA: Association for Computing Machinery, 2019, p. 211–220.

[12] Y. Shi, R. Enami, J. Wensowitch, and J. Camp, "Measurement-based characterization of LOS and NLOS drone-to-ground channels," in *IEEE WCNC*, 2018.

[13] A. Panicker, Ö. Özdemir, M. L. Sichitiu, I. Güvenç, R. Dutta, V. Marojevic, and B. A. Floyd, "AERPAW emulation overview and preliminary performance evaluation," *Elsevier Comput. Commun.*, vol. 194, p. 108083, 2021.

[14] E. Ozturk, F. Erden, and I. Guvenc, "RF-based low-SNR classification of UAVs using convolutional neural networks," *ITU J. on Future and Evolving Technol.*, vol. 2, pp. 39–52, 07 2021.

[15] M. Ezuma, F. Erden, C. Anjinappa, O. Ozdemir, and I. Guvenc, "Detection and Classification of UAVs Using RF Fingerprints in the Presence of Wi-Fi and Bluetooth Interference," *IEEE Open J. of the Commun. Soc.*, vol. 1, pp. 60–76, Nov. 2019.

[16] M. Funderburk, J. Kesler, K. Sridhar, M. L. Sichitiu, I. Guvenc, R. Dutta, T. Zajkowski, and V. Marojevic, "AERPAW vehicles: Hardware and software choices," in *Proc. of the 8th Workshop on Micro Aerial Veh. Netw., Syst., and Appl.*, 2022, pp. 37–42.

[17] QGroundControl. [Online]. Available: http://qgroundcontrol.com/

[18] ZeroMQ. [Online]. Available: https://zeromq.org/

[19] US Naval Research Laboratory. [Online]. Available: https://github.com/USNavalResearchLaboratory/mgen

[20] srsRAN. [Online]. Available: https://github.com/srsran/srsRAN

[21] 3GPP, "Non-Access-Stratum (NAS) protocol for Evolved Packet System (EPS)," Technical Specification (TS) 24.301, Apr. 2011.

[22] SRSRAN. [Online]. Available: https://github.com/anilgurses/srsRAN

[23] Karlsruhe Institute of Technology and Toyota Technological Institute at Chicago, "The KITTI Vision Benchmark Suite." [Online]. Available: http://www.cvlibs.net/datasets/kitti/

[24] A. Varischio, F. Mandruzzato, M. Bullo, M. Giordani, P. Testolina, and M. Zorzi, "Hybrid Point Cloud Semantic Compression for Automotive Sensors: A Performance Evaluation," *IEEE ICC*, 2021.

Authorized licensed use limited to: Northeastern University. Downloaded on June 26,2024 at 16:47:37 UTC from IEEE Xplore. Restrictions apply.